Electron spin resonance of carbon nanotubes under hydrogen adsorption

K. Shen,[1] D. L. Tierney,[2] and T. Pietraß[1]
[1]*Department of Chemistry, New Mexico Tech, Socorro, New Mexico 87801, USA*
[2]*Department of Chemistry, University of New Mexico, Albuquerque, New Mexico 87131, USA*
(Received 27 November 2002; revised manuscript received 13 June 2003; published 29 October 2003)

Carbon nanotubes provided by different manufacturers and synthesized by a variety of methods were subjected to the same oxidative purification procedure. Electron spin resonance (ESR) was used to investigate changes in the electronic structure before and after purification and exposure to hydrogen gas at a pressure of 136 kPa. The ESR signal in single-wall carbon nanotubes was due to paramagnetic impurities and diminished in intensity upon hydrogen adsorption. The conduction electrons of multiwall carbon nanotubes gave rise to signals with Dysonian line shapes. Here, the signal intensity increased upon hydrogen adsorption and the asymmetry parameter as well as the *g* factor were affected, suggesting a decrease in band gap. In samples with large metal content a ferromagnetic resonance was observable which disappeared upon purification. Some samples yielded no observable ESR signal due to an increased relaxation time of the electrons upon interaction with residual metal catalyst particles and possibly a large proportion of semiconducting nanotubes.

DOI: 10.1103/PhysRevB.68.165418 PACS number(s): 76.30.Pk, 76.30.Lh, 81.07.De

I. INTRODUCTION

Carbon nanotubes have been suggested as safe hydrogen storage media for fuel-cell powered vehicles.[1] The Department of Energy set the benchmark for an economically viable hydrogen storage medium to a capacity of 6.5% by weight (wt %) and a volumetric density of 63 kg H_2/m^3.[2] To date, the hydrogen uptake capacity of carbon nanotubes is still contested, and reports from experimental and theoretical studies cover a wide range.[3–6] The nature of the sorption mechanism is also unclear.[7,8] With three major production methods (laser ablation, chemical vapor deposition, and electric arc discharge) as well as numerous chemical and mechanical purification methods, the identity of samples investigated by different researchers is expected to vary considerably and thus, to impact the results. Most hydrogen adsorption experiments rely on macroscopic techniques such as volumetric or mass uptake measurements, thermal gravimetric analysis (TGA), or temperature programmed desorption.[3,6,9] Spectroscopic tools have been used in the characterization of carbon nanotubes, although rarely for the study of hydrogen adsorption.[10,11] We use electron spin resonance spectroscopy to study both the effect of purification and of hydrogen adsorption on the electronic structure of carbon nanotubes. In this study, we examine single-walled and multiwalled carbon nanotube samples manufactured with different methods.

II. EXPERIMENT

A summary of the samples is provided in Table I. Prior to ESR experiments, the samples were weighed into J. Young sample tubes made from low impurity synthetic quartz (''Suprasil,'' Wilmad) and heated for 12 h at 400 °C under high vacuum in order to desorb any contaminants. All samples were studied as received and after an oxidative purification procedure.[12] The samples were characterized by inductively coupled plasma/mass spectrometry (ICP-MS) from the solution phase before and after purification and visually inspected using transmission electron microscopy (TEM). For most samples, the metal content decreased significantly upon purification (see Table I). Two samples (CNI and CLex) showed an impossible metal content of more than 100 wt % which is related to the high viscosity of the solution in the filtration process. While the metal content could not be quantitated for these samples, it must be very high in agreement with the information provided by the manufacturers. Resonant Raman experiments for the distinction between metallic and semiconducting tubes[13] were not conclusive due to limitations of the instrument used. Electron spin resonance (ESR) data were recorded on a Bruker EMX ESR spectrometer at a typical microwave frequency of 9.4 GHz and a microwave power of 0.152 mW. The modulation amplitude was 5 G and the time constant 10 ms. Spectra for all samples were recorded applying both a wide scan covering a range of 8000 G and a narrow scan of 200 G centered at $g=2$. All ESR data were acquired using an Oxford liquid He cryostat at temperatures of 3.8–4.0 K. It should be noted that many of our samples (with the exception of MRGC and CNI) caused the quality factor of the resonant cavity to decrease. A proper adjustment of the microwave bridge was then not possible which may cause distortions of the line shapes. A similar effect has been reported by Bandow.[14] For the hydrogen adsorption studies, the samples were exposed for 5 min at ambient temperature to a hydrogen (UHP grade, Matheson-Trigas) pressure of 136 kPa inside the sealed ESR tube.

III. RESULTS AND DISCUSSION

A. General

In general, ESR signals from carbon nanotubes should be observable for localized spins due to impurities, and for conduction electrons originating from metallic or semiconducting nanotubes with a small band gap. In addition to conduction electron spin resonance (CESR) from metallic and graphitic particles,[15] a ferromagnetic resonance (FMR) may also be present due to residual metallic catalyst particles.[16,17]

TABLE I. Sample characteristics. All entries except the ICP data are as provided by the manufacturer. Carb. Nano.=Carbon Nanotechnologies, CAD=carbon arc discharge. ICP-MS data are given in $g_{metal}/g_{rawmaterial}$; Met. Imp.=Metal Impurities, ICP-MS Pur. =ICP-MS results after purification.

Sample	Manufact.	Prod. method	Structure	Length (μm)	Diam. (nm)	Pur.	Met. Imp.	ICP-MS (wt %)	ICP-MS Pur. (wt %)
MRSW	Mer Corp.	CAD	single wall, open	up to 100	1.3	>90%	Co, Ni	32	15
CLex	Carbolex	CAD	single wall, closed	2–5	1.4, 50 tb./rope	50–70%	Ni, Yt	112	260
CNI	Carb. Nano.	HiPco	single wall [a]	0.1–1	1	<72%	Fe 25%	169	20
CNI pur.	Carb. Nano.	HiPco	single wall [a]	0.1–1	1	91%	Fe 9%	76	N/A
MRMWC	Mer Corp.	CVD	multi wall, closed	50	N/A	>95%	Fe <0.1%	4	3
MRGC	Mer Corp.	CAD	multi wall, closed	N/A	50	N/A	none	1	0.3
NL15	Nanolab	CVD	multi wall, open	1–5	20–50	95%	Fe	12	13
NL1020	Nanolab	CVD	multi wall, open	10–20	20–50	95%	Fe	13	14
NLbamboo	Nanolab	N/A	bamboo, open	N/A	N/A	95%	Fe	2	4

[a]The manufacturer did not provide information about tube ends.

The line shapes may vary from symmetric (Lorentzian/Gaussian) to asymmetric (Dysonian).[18]

A narrow resonance is expected for isolated single-walled carbon nanotubes that lack interchain interactions since most of the spin-relaxation mechanisms typical for isotropic metals (spin-flip scattering of conduction electrons by acoustic phonons) are absent.[19] However, no CESR signal has been observed in single-walled carbon nanotubes. In very pure samples, this might be due to the strong electron-electron correlation in a one-dimensional system, giving rise to an antiferromagnetic ground state. However, even a small amount of residual catalyst metal can relax the conduction electrons very effectively due to their long mean free path and diffusion length.[19]

The higher dimensionality of the electronic system in multiwalled carbon nanotubes provides a less efficient relaxation pathway in the presence of metal particles and makes the CESR more likely to be observed. Theoretical calculations, however, predict a single narrow peak for multiwalled nanotubes, and a split resonance for single-walled tubes[20] which has not been observed yet. Most likely, samples of sufficient quality are not available to corroborate the theoretical result. Some carbon nanotube samples do not give rise to any ESR signal. For example, Chen *et al.*[21] were unable to observe a signal for a pristine, unpurified Carbolex sample in agreement with our results. Claye *et al.*[17] report the lack of an ESR resonance of highly purified single-walled carbon nanotubes in the form of buckypaper unless they were doped with potassium. The presence of Ni, however, gave rise to a ferromagnetic resonance. The authors conclude that the spin lifetime, which is expected to be long on a light element such as carbon, must be dominated by Ni particles. The spin diffusion time of the electrons is longer than the average distance between the Ni atoms, resulting in a broadening of the CESR due to coupling to the FMR. Potassium doping causes a decoupling of the resonances due to shortening of the spin relaxation time.

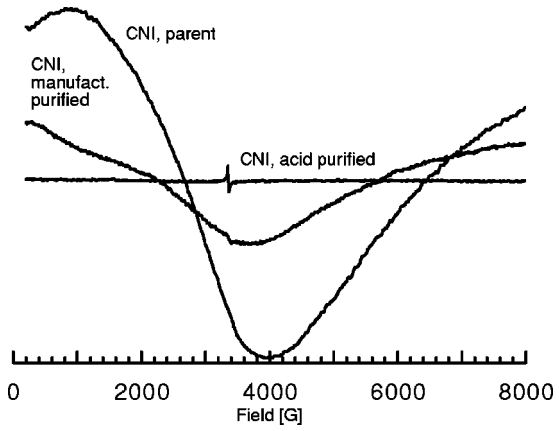

FIG. 1. ESR spectra of CNI samples; parent, manufacturer purified, and acid purified.

B. Single-walled carbon nanotubes (SWNT's)

1. Parent materials, effect of production method

A ferromagnetic resonance due to the high residual metal content was detected in all three single-walled samples. The strongest resonance was observed for the CNI sample with the highest metal content (Table I, Fig. 1). The weakest resonance for the MRSW sample with the smallest metal content. The approximate g factors of 2.6 (CLex) and 2.5 (CNI) for the FMR are in reasonable agreement with the g factors for metallic Fe and Ni.[22] When reducing the sweep width to 200 G centered around $g=2.0$, a weak, symmetric resonance became visible for the MRSW sample, produced by carbon arc discharge. Despite the application of the same production method, no such signal was observable for CLex, in agreement with the results by Chen *et al.*[21] The parent CNI material, produced by the HiPco process (high-pressure injection of CO), did not give rise to an ESR signal either. It seems that there is no correlation between the appearance of an ESR signal and the production method. Any differences due to production method are masked by the FMR that arises from the very high metal content (more than 30 wt %) in all our SWNT's.

2. Effect of purification

The oxidative treatment caused the FMR to disappear in all three single-walled samples, consistent with the greatly

reduced metal content detected by ICP-MS (Table I). It should be noted that the measurement of the metal content provided by the manufacturer using TGA differed significantly from ours determined using ICP-MS. In general, the ICP-MS method measured higher metal contents than those reported by the manufacturers. This may be due to the fact that our ICP-MS pretreatment completely disintegrates the carbon network (the residue after oxidation is acid soluble) so that any metal, even that which is contained within the nanotubes, is accessible to analysis. Moreover, the CLex sample showed a very high metal content both before and after the purification.

The manufacturer purified CNI sample shows a reduction of the FMR when compared to the parent material. The manufacturer used a nondisclosed oxidative purification method which was not as effective as our nitric acid purification procedure following the method by Dillon *et al.*[12] (Fig. 1). Upon purification, the narrow, symmetric resonance previously observed for MRSW is now observable in all samples. No obvious shift in g factor occurred for MRSW. The g factors for all SWNT samples were close to 2.00, in agreement with g factors of 2.00–2.01 reported by most researchers.[14,16,17,21,23–29] It should be noted that the anisotropy in the g factor for graphite ranges from $g_{\perp}=2.0026$ to $g_{\parallel}=2.0496$.[15] Even after purification, all SWNT samples still had metal contents larger than 20%. A large metal content is known to cause rapid relaxation of the conduction electrons rendering most of the nanotubes unobservable.[19] The harsh purification conditions cause partial exfoliation of the tubes as evidenced by TEM and are expected to increase the number of defect sites. The rather weak and symmetric resonances observed for the purified samples and the increase in signal intensity after purification imply that the signals originate from paramagnetic defects such as dangling bonds. Unlike graphite, a symmetric resonance assigned to dangling bonds has also been observed for fullerene soots.[30]

3. Effect of hydrogen exposure

Despite the close to ambient pressures that were applied, hydrogen exposure had a pronounced effect on the ESR spectra. No difference was observable between single-walled and multiwalled samples investigated immediately after hydrogen exposure and 24 h later, indicating that equilibrium conditions are established rapidly. A pronounced decrease in signal intensity is observed for all SWNT's. For example, the intensity of the narrow resonance of the acid purified CNI sample is diminished upon hydrogen adsorption (Fig. 2) while the g factor as well as the symmetric line shape remain unaffected. For the manufacturer purified CNI sample, the ferromagnetic resonance shifted 650 G to higher field upon hydrogen exposure, while the carbon nanotube resonance shifted by 8 G in the same direction, possibly indicating a coupling of the two resonances. The large shift of the ferromagnetic resonance clearly shows the interaction of hydrogen with the metal. Similarly for CLex, the signal intensity is greatly diminished upon hydrogen adsorption and the resonance shifts to slightly lower field. The attenuation of the resonance upon hydrogen adsorption suggests that hydrogen preferentially adsorbs on defect sites consistent with our hypothesis that the ESR resonance is mainly due to paramagnetic defects. A similar observation has been made on mechanically prepared nanostructured graphite.[31] Moreover, it has been shown that hydrogenation in polycrystalline silicon diminished the density of dangling bonds and led to a decrease in the ESR signal intensity.[32–36]

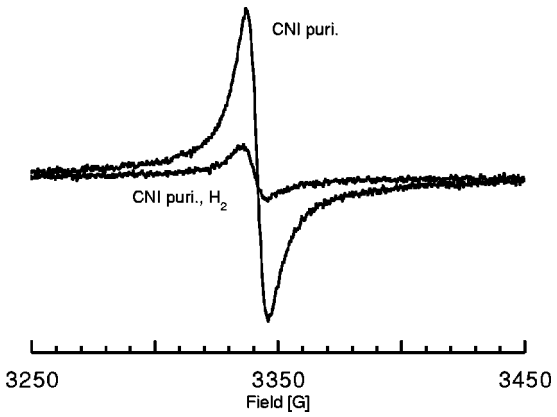

FIG. 2. ESR spectra of acid purified CNI sample before and after hydrogen adsorption.

C. Multiwalled carbon nanotubes

1. Parent materials, effect of production method

None of the Nanolab parent materials, all prepared by chemical vapor deposition, gave rise to an ESR signal. However, for both samples from the MER corporation, MRGC (carbon arc discharge without metal catalyst) and MRMWC (chemical vapor deposition), strong ESR signals were observed. The metal content in all these samples is considerably less than for the SWNT's and, as expected, no FMR is detected. A single, slightly asymmetric resonance ($A/B=1.20$, Fig. 3) is observed for MRMWC, while the MRGC parent material displays a narrow signal superimposed upon a broad resonance at lower field (Fig. 4).

Graphitic particles have been reported to have g factors of about 2.02 with linewidths of 10–25 G. As mentioned above,

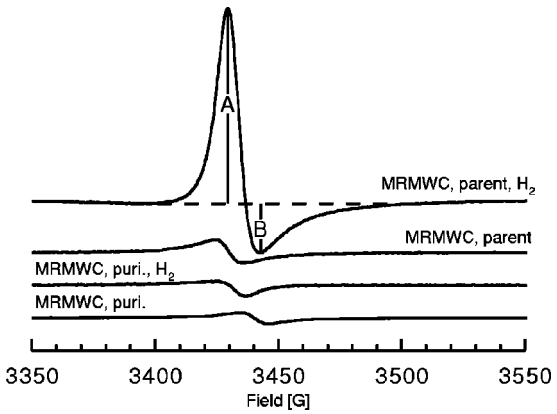

FIG. 3. ESR spectra of MRMWC samples; parent and purified material, before and after hydrogen adsorption. The parameters A and B are related to the ratio of the particle radius r to the skin depth δ (see text) (Ref. 46 and 47).

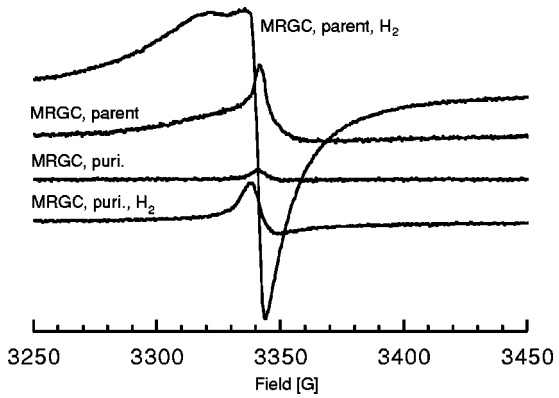

FIG. 4. ESR spectra of MRGC samples; parent and purified material, before and after hydrogen adsorption.

most *g* factors assigned to carbon nanotubes are in the range 2.00–2.01 with varying linewidths of the order of a few Gauss.[37] Therefore, tentatively, the broader resonance in the MRGC spectrum is assigned to graphitic particles. Indeed, particles are visible in the TEM pictures which cannot be metallic since MRGC was prepared without a metal catalyst. Rings in the TEM diffraction pattern indicate that most of these particles are polycrystalline and, therefore, most likely graphitic in nature.

TEM micrographs of the MRMWC sample reveal a high content of carbon nanotubes with very few graphitic particles, in agreement with the single line observed in the ESR spectrum.

As for the SWNT's, no direct correlation between ESR signature and production method can be drawn. While both MRMWC and NL were synthesized using chemical vapor deposition, no ESR signal was obtained for any of the NL samples. The NL samples have a considerably higher metal content which might lead to fast relaxation of conduction electrons rendering the signal unobservable. Nevertheless, the metal content of the NL samples is much smaller than for any of the SWNT samples and not sufficient for observation of FMR. Moreover, dangling bonds cannot be prevalent. Dysonian line shapes were observed for samples prepared by chemical vapor deposition and carbon arc discharge. Multiple reports about multiwalled, carbon arc discharge produced carbon nanotubes also report ESR signals due to conduction electrons.[19,23,28,29,38,39] Overall, the metal content and the presence of graphitic particles seem to have the dominating effect on spectral appearance. The ESR signal originates from conduction electrons, as evidenced by the asymmetric line shapes.

2. Effect of purification

For all samples grown with chemical vapor deposition, the metal content is, within error, not reduced upon acid purification. This implies that metal particles must be inaccessible to acid, and possibly be contained within the nanotubes. Indeed, the NL TEM pictures show the presence of particles embedded in the nanotubes (Fig. 5) which is common for chemical vapor deposition (CVD) grown tubes.[40] Upon purification, these tubes broke into smaller pieces, accompanied by exfoliation of the outer layers.[41] Carbon nanotubes grown with the CVD process may be particularly prone to exfoliation due to their less well-defined graphene structure brought about by the lower temperature in the growth process, as compared to arc discharge or laser ablation.[40] The TEM pictures of the NL samples reveal the presence of larger diameter nanotubes with bamboo structure (compare NLbamboo, Table I) which are predominant in the NL15 sample. These larger tubes seem to be less affected by purification than the smaller diameter concentric tubes. The absence of a ^{13}C NMR signal for all but the unpurified NL15 and NL1020 samples suggests that the ^{13}C NMR signal originates from the smaller diameter tubes.[42] If metal particles are contained within the nanotubes, as implied by the ICP-MS and suggested by the TEM, then the ^{13}C NMR signal may be paramagnetically broadened beyond detectability. Previous work has shown that a small amount of paramagnetic contaminant is sufficient for the resonance to disappear.[43]

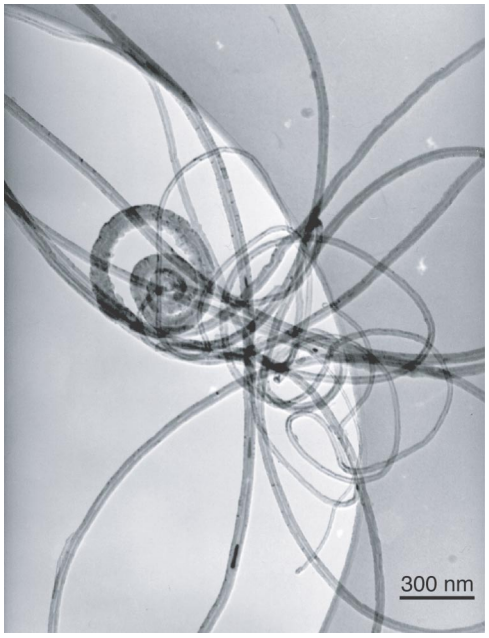

FIG. 5. TEM micrograph of NL1020 sample before acid purification. Note the particles embedded in the interior of the tubes.

For MRMWC, purification caused a slight decrease in signal intensity, a shift by 8 G to lower field, and a change to a symmetric line shape. TEM pictures reveal severe damage to the tube walls. Therefore it is possible that the changes in the ESR spectrum are due to the fact that predominantly defect sites are being observed.

The broad resonance in MRGC which had been assigned to graphitic particles disappears upon purification in agreement with the TEM results.

3. Effect of hydrogen exposure

No signal was observed for the Nanolab samples before and after exposure to hydrogen. However, hydrogen adsorption drastically *increases* the intensity of both the narrow and the broad signal components in the parent MRGC material.

In the purified material, a large increase in the signal intensity as well as a shift of the resonance to lower field is observed (Fig. 4). The line shape for the purified sample after hydrogen adsorption is clearly Dysonian with an increased asymmetry $A/B=3.28$ and increased linewidth (see Fig. 4). Line broadening upon hydrogen exposure has also been observed for hydrogen passivated, phosphorus doped crystalline silicon and was assigned to the Fermi-contact hyperfine interaction of the donor with silicon.[32] The line shape of the MRGC parent material after hydrogen exposure is very asymmetric, which might reflect saturation of the receiver, as a faster scan rate led to a more symmetric line shape. The Dysonian line shape indicates that a large fraction of the nanotubes must be metallic. The MRGC samples were produced without a metal catalyst and the interaction of hydrogen with metallic particles cannot account for the increase in line intensity. A possible explanation for the observed increase is a decrease in band gap, such that semiconducting tubes previously unobservable may become accessible to ESR. This explanation is in agreement with the more pronounced Dysonian line shape (a larger fraction of the signal is now due to CESR from nanotubes). Indeed, theoretical work shows that hydrogen adsorption on single-walled radially deformed carbon nanotubes causes the energies of the valence band edge and conduction band edge to change such that the overall band gap is decreased for zigzag nanotubes.[44,45] It should be noted, however, that for some tubes the opposite trend was observed.

If this interpretation is correct, an increase in the signal intensity upon hydrogen adsorption should be observed for all metallic nanotubes giving rise to a Dysonian line shape. In fact, a strong increase in signal intensity is also observed for the MRMWC parent sample (Fig. 3). The line shape becomes more asymmetric upon hydrogen adsorption. The effect of hydrogen exposure on the purified MRMWC sample is less pronounced. The change in g factor and in line shape indicate that the defect sites have been saturated by hydrogen, and conduction electrons become again observable.

Following the analysis by Feher and Kip[46] and Webb,[47] the asymmetry A/B (see Fig. 3) is related to the ratio of the particle radius r to the skin depth δ. For A/B close to 1, δ must be larger than or equal to r. For MRMWC, $A/B=3.45$ after hydrogen adsorption which corresponds to a ratio of r/δ of about 2.5.[47] From conductivity measurements, Petit *et al.* found a skin depth for SWNT's at room temperature of about 50 μm;[48] the room temperature value for graphite is 3.2 μm.[15] A particle size in the μm range for carbon nanotubes can only be realized along the tube axis which implies that conduction occurs mainly along the tube axis, in agreement with the result by Petit.[48]

For MRMWC, the observed ESR linewidths lie in the range of 11–13 G corresponding to a relaxation time of about 10–9 ns at 4 K. The diffusion time through the skin depth, T_D, can be estimated from the asymmetry A/B and the linewidth following the analysis of Feher and Kip.[46] For the MRMWC parent material, T_D is estimated to be 0.02 ns before hydrogen adsorption, whereas after hydrogen exposure T_D increases to about 2 ns. This implies a significant increase in the skin depth brought about by hydrogen adsorption which should induce an increase in the signal amplitude, in agreement with the experimental result. Hydrogen adsorption on MRMWC showed a shift to higher field. In this sample, the signal has been ascribed to CESR where the g factor is determined by the spin-orbit coupling of the energy levels in the presence of a magnetic field. Since the conduction electrons in carbon nanotubes reside in p-type orbitals which possess orbital angular momentum, a coupling of these electrons to hydrogen via physi- or chemisorption is expected to impact the spin-orbit coupling resulting in a shift of the g factor, as observed. In fact, hydrogen adsorption causes the character of bonding to change locally[44] from sp^2 to sp^3 which should affect the spin-orbit coupling. Further experiments with varying hydrogen pressure are planned to shed light on this hypothesis.

IV. CONCLUSIONS

In conclusion, the exposure of carbon nanotubes to hydrogen affects the electron spin resonance signal. In single-walled carbon nanotubes, we observed a paramagnetic resonance signal due to impurities which present favorable adsorption sites to hydrogen. Consequently, the ESR signal is diminished upon hydrogen adsorption. Multi-walled carbon nanotubes, where the CESR of delocalized π electrons is observable, presented a Dysonian line shape. Hydrogen adsorption increased the signal intensity and affected both the asymmetry parameter and g factor, giving evidence for the interaction of hydrogen with the tube surface. We used analysis of the line shape in combination with TEM and ICP data for the assignment of the resonances. ESR experiments as a function of temperature are planned to support these assignments. The magnetic susceptibility due to conduction electrons is temperature independent while isolated, random spins follow the Curie law. Variable pressure experiments are planned to investigate the effect of hydrogen pressure on g factor and line shape.

ACKNOWLEDGMENTS

This material was based upon work supported by the National Science Foundation under Grant No. 0107710.

[1] A.C. Dillon, K.M. Jones, T.A. Bekkedahl, C.H. Klang, D.S. Bethune, and M.J. Heben, Nature (London) **386**, 377 (1997).

[2] S. Hynek, W. Fuller, and J. Bentley, Int. J. Hydrogen Energy **22**, 601 (1997).

[3] R.G. Ding, G.Q. Lu, Z.F. Yan, and M.A. Wilson, J. Nanosci. Nanotechnol. **1**, 7 (2001).

[4] M.S. Dresselhaus, K.A. Williams, and P.C. Eklund, MRS Bull. **24**, 45 (1999).

[5] L. Schlapbach and A. Züttel, Nature (London) **414**, 353 (2001).

[6] H.-M. Cheng, Q.-H. Yang, and C. Liu, Carbon **39**, 1447 (2000).

[7] R. Dagani, Chem. Eng. News **80**, 25 (2002).
[8] V.V. Simonyan and J.K. Johnson, J. Alloys Compd. **330**, 659 (2002).
[9] A.C. Dillon and M.J. Heben, Appl. Phys. A: Mater. Sci. Process. **A72**, 133 (2001).
[10] M. Schmid, S. Krämer, M. Mehring, S. Roth, M. Haluska, and P. Bernier, AIP Conf. Proc. **591**, 598 (2001).
[11] M. Schmid, S. Krämer, C. Goze, M. Mehring, S. Roth, and P. Bernier, Synth. Met. **135-136**, 727 (2003).
[12] A.C. Dillon, T. Gennett, K.M. Jones, J.L. Alleman, P.A. Parilla, and M.J. Heben, Adv. Mater. (Weinheim, Ger.) **11**, 1354 (1999).
[13] M.A. Pimenta, A. Marucci, S.D.M. Brown, M.J. Matthews, A.M. Rao, P.C. Eklund, R.E. Smalley, G. Dresselhaus, and M.S. Dresselhaus, J. Mater. Res. **13**, 2396 (1998).
[14] S. Bandow, S. Asaka, X. Zhao, and Y. Ando, Appl. Phys. A: Mater. Sci. Process. **A67**, 23 (1998).
[15] G. Wagoner, Phys. Rev. **118**, 647 (1960).
[16] A. Thess, R. Lee, P. Nikolaev, H. Dai, P. Petit, J. Robert, C. Xu, Y.H. Lee, S.G. Kim, A.G. Rinzler, D.T. Colvert, G.E. Scuseria, D. Tomnek, J.E. Fischer, and R.E. Smalley, Science **273**, 483 (1996).
[17] A.S. Claye, N.M. Nemes, A. Jánossy, and J.E. Fischer, Phys. Rev. B **62**, R4845 (2000).
[18] F.J. Dyson, Phys. Rev. **98**, 349 (1955).
[19] L. Forró and C. Schönenberger, Top. Appl. Phys. **80**, 329 (2001).
[20] A. De Martino, R. Egger, K. Hallberg, and C.A. Balseiro, Phys. Rev. Lett. **88**, 206402 (2002).
[21] Y. Chen, J. Chen, H. Hu, M.A. Hamon, M.E. Itkis, and R.C. Haddon, Chem. Phys. Lett. **299**, 532 (1999).
[22] S. Chikazumi, *Physics of Magnetism* (Wiley, New York, 1964).
[23] A.S. Kotosonov and D.V. Shilo, Carbon **36**, 1649 (1998).
[24] O. Chauvet, G. Baumgartner, M. Carrard, W. Bacsa, D. Ugarte, W.A. deHeer, and L. Forró, Phys. Rev. B **53**, 13 996 (1996).
[25] O. Chauvet, L. Forró, W. Bacsa, D. Ugarte, B. Doudin, and W.A. deHeer, Phys. Rev. B **52**, R6963 (1995).
[26] S. Bandow, J. Appl. Phys. **80**, 1020 (1996).
[27] F. Beuneu, C. l'Huillier, J.-P. Salvetat, J.-M. Bonard, and L. Forró, Phys. Rev. B **59**, 5945 (1999).
[28] M. Kosaka, T.W. Ebbesen, H. Hiura, and K. Tanigaki, Chem. Phys. Lett. **225**, 161 (1994).
[29] M. Kosaka, T.W. Ebbesen, H. Hiura, and K. Tanigaki, Chem. Phys. Lett. **233**, 47 (1995).
[30] J. Dunne, A.K. Sarkart, H.W. Kroto, J. Munn, P. Kathirgamanathan, U. Heinen, J. Fernandez, J. Hare, D.G. Reid, and A.D. Clark, J. Phys.: Condens. Matter **8**, 2127 (1996).
[31] S. Orimo, T. Matsushima, H. Fujii, T. Fukunaga, and G. Majer, J. Appl. Phys. **90**, 1545 (2001).
[32] K. Murakami, H. Suhara, S. Fujita, and K. Masuda, Phys. Rev. B **44**, 3409 (1991).
[33] M. Stutzmann and D.K. Biegelsen, Phys. Rev. B **40**, 9834 (1989).
[34] S. Hasegawa, K. Kishi, and Y. Kurata, J. Appl. Phys. **55**, 542 (1984).
[35] N. Fukata, S. Sasaki, S. Fujimura, H. Haneda, and K. Murakami, Jpn. J. Appl. Phys., Part 1 **35**, 3937 (1996).
[36] M. Kumeda and T. Shimizu, Jpn. J. Appl. Phys. **19**, L197 (1980).
[37] J.N. Coleman, D.F. O'Brien, A.B. Dalton, B. McCarthy, B. Lahr, R.C. Barklie, and W.J. Blau, J. Chem. Phys. **113**, 9788 (2000).
[38] P. Byszewski and A. Nabialek, Europhys. Lett. **34**, 31 (1996).
[39] Y.-H. Lee, H. Kim, D.-H. Kim, and B.-K. Ju, J. Electrochem. Soc. **147**, 3564 (2000).
[40] S.B. Sinnott and R. Andrews, Crit. Rev. Solid State Mater. Sci. **26**, 145 (2001).
[41] N. Yao, V. Lord, S.X.C. Mao, E. Dujardin, A. Krishnan, M.M.G. Treacy, and T.W. Ebbeson, J. Mater. Res. **13**, 2432 (1998).
[42] K. Shen and T. Pietraß (unpublished).
[43] J.M. Kneller, R.J. Soto, S.E. Surber, J.-F. Colomer, A. Fonseca, J.B. Nagy, G.v. Tendeloo, and T. Pietraß, J. Am. Chem. Soc. **122**, 1059 (2000).
[44] O. Gülseren, T. Yildirim, and S. Ciraci, Phys. Rev. Lett. **87**, 116802 (2001).
[45] O. Gülseren, T. Yildirim, and S. Ciraci, Phys. Rev. B **66**, 121401(R) (2002).
[46] G. Feher and A.F. Kip, Phys. Rev. **98**, 337 (1955).
[47] R.H. Webb, Phys. Rev. **158**, 225 (1967).
[48] P. Petit, E. Jouguelet, J.E. Fischer, A.G. Rinzler, and R.E. Smalley, Phys. Rev. B **56**, 9275 (1997).